



Calhoun: The NPS Institutional Archive
DSpace Repository

Theses and Dissertations

1. Thesis and Dissertation Collection, all items

1973

Sound radiation from line arrays.

Akst, H. Gordon.

Massachusetts Institute of Technology

<https://hdl.handle.net/10945/16814>

Downloaded from NPS Archive: Calhoun



Calhoun is the Naval Postgraduate School's public access digital repository for research materials and institutional publications created by the NPS community. Calhoun is named for Professor of Mathematics Guy K. Calhoun, NPS's first appointed -- and published -- scholarly author.

Dudley Knox Library / Naval Postgraduate School
411 Dyer Road / 1 University Circle
Monterey, California USA 93943

<http://www.nps.edu/library>

SOUND RADIATION FROM LINE ARRAYS.

H. Gordon Akst

LIBRARY
NAVAL POSTGRADUATE SCHOOL
MONTEREY, CALIF. 93940

SOUND RADIATION FROM LINE ARRAYS

by

H. GORDON AKST

B.S., United States Naval Academy

1966

SUBMITTED IN PARTIAL FULFILLMENT OF
THE REQUIREMENTS FOR THE DEGREE OF
MASTER OF SCIENCE IN NAVAL ARCHITECTURE AND
MARINE ENGINEERING AND
THE PROFESSIONAL DEGREE OF
OCEAN ENGINEER

at the

MASSACHUSETTS INSTITUTE OF TECHNOLOGY

June 1973

Abstract

Title: Sound Radiation from Line Arrays

Author: H. Gordon Akst

Submitted to the Department of Ocean Engineering on 11 May 1973
in partial fulfillment of the requirements for the degree of Master
of Science in Naval Architecture and Marine Engineering and the
professional degree of Ocean Engineer.

This paper develops simple approximations for the sound
radiation of the accordion (longitudinal) and the whipping (trans-
verse) vibration of a spheroid. This analysis can be directly
applied to the fundamental vibratory modes of a submarine hull.
The very close correlation between these predictions and the
exact spheroidal wave functions is demonstrated for far-field
radiation from a slender spheroid. This correlation is carried out
over the ranges of angular position and frequency of practical
interest. Through application of these approximations in future
predictions, the use of the cumbersome spheroidal wave functions
can be avoided.

Thesis Supervisor: Miguel C. Junger

Title: Senior Lecturer, Department of Ocean Engineering (Visiting)

Acknowledgement

I should like to thank Dr. Miguel Junger for his time and patience during the preparation of this paper. His uncanny ability to quickly detect errors and recommend improvements in my work has been of great help. Furthermore, my personal benefit from this study has been enhanced by the physical insight he has injected into it.

I am also indebted to the Department of Ocean Engineering for provision of numerical calculation facilities and to Pam Llewellyn for typing.

Table of Contents

Abstract

Acknowledgement

Table of Contents

I. Introduction

II. Procedure

III. Accordion Mode Approximation

IV. Accordion Mode Spheroidal Calculation

Figure 1 Accordion Mode Pressure vs. Frequency

Figure 2 Accordion Mode Pressure vs. Frequency

Table I Accordion Mode Results

V. Whipping Mode Approximation

VI. Whipping Mode Spheroidal Calculation

Figure 3 Whipping Mode Pressure vs. Angle ($h = 2$)

Figure 4 Whipping Mode Pressure vs. Angle ($h = 4$)

Table II Whipping Mode Results

VII. Near Field Approximations

Figure 5 Accordion Mode Pressure vs. Distance

Figure 6 Whipping Mode Pressure vs. Distance

Table III Near Field Results

VIII. Summary and Conclusions

Appendix A Spheroidal Wave Functions

Appendix B Near Field Numerical Calculations

Appendix C Important Symbols

Appendix D Bibliography

SOUND RADIATION FROM LINE ARRAYS

I. Introduction

The purpose of this paper is to develop simple approximations for the sound radiated from slender spheroidal bodies. The analysis of such bodies can be directly applied to the fundamental modes of submarine hulls and is therefore of practical interest in the field of naval architecture. Although the technique can be extended to any mode, this paper will deal only with the accordion and whipping modes, which are of the most practical interest.

Although exact spheroidal radiation can be predicted from the available literature, the wave functions involved are unfamiliar and cumbersome. In addition to the inherent complication of the functions themselves, each author who deals with them tends to select his own notation, further exasperating the novice in their use. One significant result of this study has been my familiarity with these functions, however slowly and painfully acquired. I have also gained an appreciation of the desire to replace these functions by more convenient predictions, which is the express purpose of this investigation. If one future investigator of such radiation is spared the use of spheroidal functions, this study will have fulfilled its purpose. However, since spheroidals form the exact answer that this paper is attempting to approximate, their use is mandatory to demonstrate the validity of those approximations. A brief summary of the necessary properties of spheroidal wave functions is included in Appendix A.

Literature on spheroidal functions is relatively complete. C. Flammer¹ and J. A. Stratton² have both published tables of spheroidal functions, but neither is ideal. Although containing all the required data, Flammer's tables are of rather limited range, and Stratton publishes only the expansion coefficients, requiring calculation of the other data from them. G. Chertock's³ paper includes a concise and useful summary of the functions and analyzes some properties of individual spheroidal modes for rigid body axial vibration and accordion mode vibration. These analyses are reproduced in E. Skudrzyk's⁴ chapter on spheroidal functions, along with a complete and detailed development of spheroidal properties. A combination of all these sources was required to overcome the shortcomings of each individually and the variance in notation between them.

As mentioned previously, this paper will develop approximations for the total sound radiation from the accordion and whipping modes of a slender spheroidal shell. Chertock's accordion results are for individual modes only, and not for the total radiation. M. Strasberg⁵ has investigated the accordion mode radiation without Poisson effect, but demonstrates only fair agreement at higher frequencies. W. Blake⁶ has analytically predicted the acoustic radiation from the transverse motion of a long, slender beam with elliptical cross section. Finally,

¹C. Flammer, Spheroidal Wave Function (Stanford, 1957).

²J. A. Stratton, et al., Spheroidal Wave Functions (Cambridge, 1956).

³C. Chertock, "Sound Radiation From Prolate Spheroids," JASA 33(1961)871.

⁴E. Skudrzyk, The Foundations of Acoustics (New York, 1971).

⁵M. Strasberg, "Sound Radiation from Slender Bodies in Axisymmetric Vibrations," Fourth International Congress on Acoustics, 1962.

⁶W. K. Blake, "Radiation from Free-Free Beams Under Influences of Light and Heavy Fluid Loading," NSRDC Report 3716 (1971).

M. Junger⁷ has formulated the basis for the whipping mode approximation developed in this study. This paper will extend the results of Strasberg and Junger and verify those results with the exact spheroidal radiation.

⁷M. C. Junger, "Sound Radiation by Resonances of Free-Free Beams," JASA 52 (1972); 332,

II. Procedure

In general, the procedure followed by this paper will be to formulate an approximation of sound radiated from a spheroid by utilizing line arrays of sources with varying strength along the line. For the accordion mode, which is the longitudinal vibration of a body, the appropriate source type is the simple source; while for the whipping mode or transverse vibration, a dipole source is applicable. Higher modes can be similarly approximated by line arrays of multipole sources. This approximation is then compared with its spheroidal equivalent.

The first step of the approximation is definition of the shape and certain properties of the radiating body in both cartesian and spheroidal coordinates. Since the body used is a spheroid or an ellipsoid of revolution, this step is basic. The next step is to formulate the incremental radiation from an element of length dz along the axis of the radiator. Such formulations are available from basic theory of sound sources. A surface velocity distribution is then selected that approximates the mode under investigation, and from it, the source strength is determined as a function of position on the axis. Finally, the incremental radiation is integrated along the length of the body, and an expression for the total radiation is obtained.

The exact spheroidal radiation is determined as a summation of the individual spheroidal mode radiations. The acoustic pressure is related to the normal velocity, and the modal pressure coefficients are determined. Their evaluation is accomplished by matching the -velocity expression to the prescribed velocity distribution over the

body and utilizing the orthogonality of the angle functions. The resulting integrals are then evaluated, and approximations for far-field and slender body are applied, resulting in expressions for each mode. These are summed to obtain total radiation.

In principle, both formulations are straightforward but are complicated in practice by difficult integrations and infinite summations. Evaluation of the resulting expressions is also cumbersome, involving extensive numerical manipulations. As will be pointed out later, some effort must be devoted to maintain precision, if fictitious peaks in the smooth functions are to be avoided.

Since the two methods are obviously considerably different, the arrival at equivalent expressions fortunately is an indication that both are probably correct.

III. Accordion Mode Approximation

As pointed out in the procedure section, the first step in the formulation of the problem is to develop certain properties of the radiating body, in this case, a spheroid. The expressions developed will be used in both the accordion and whipping mode approximations.

For an ellipse of focal length d , major axis L , and minor axis D , $d^2 = L^2 (1 - (D/L)^2)$, as shown in Appendix A. Therefore, for slender spheroids ($D \ll L$), d is approximately equal to L . For purposes of this discussion, the other properties of interest can be derived for the ellipse that is the intersection of the spheroid and the x - z plane. In this case, x is the perpendicular distance to the axis and z is the distance along the axis with $z = 0$ at the center of the body. The governing equation for this ellipse is:

$$\frac{z^2}{(L/2)^2} + \frac{x^2}{(D/2)^2} = 1$$

If $a(z)$ is defined as the radius of the cross-sectional area normal to the axis, then:

$$a(z) = x(z) = D\left(\frac{1}{4} - (z/L)^2\right)^{1/2} \quad (1)$$

If $\alpha(z)$ is the angle between the normal to the spheroid and the normal to the z axis, then:

$$\tan(\alpha(z)) = - dx/dz = \frac{Dz}{L^2\left(\frac{1}{4} - (z/L)^2\right)^{1/2}} \quad (2)$$

Using that definition of $\alpha(z)$, the normal velocity of the spheroidal surface is made up of contributions from both the axial and "radial" (perpendicular to axial) velocities as follows:

$$u_n = u_z \sin(\alpha(z)) + u_r \cos(\alpha(z)) \quad (3)$$

For the array approximation, only the tangent form is required; however, for the spheroidal work, the individual sine and cosine terms must be obtained. Using:

$$\sin(\alpha(z)) = \frac{-dx}{((dx)^2 + (dz)^2)^{1/2}}$$

$$\cos(\alpha(z)) = \frac{dz}{((dx)^2 + (dz)^2)^{1/2}}$$

and differentials obtained from Skudrzyk's expressions⁸ leads to the following relationships for the spheroidal velocities:

$$\sin(\alpha(\eta)) = \eta \left[\frac{\xi_o^2 - 1}{\xi_o^2 - \eta^2} \right]^{1/2} \quad (4)$$

$$\cos(\alpha(\eta)) = (L/D) (1 - \eta^2)^{1/2} \left[\frac{\xi_o^2 - 1}{\xi_o^2 - \eta^2} \right]^{1/2} \quad (5)$$

Finally, the incremental surface area along length dz is given by:

$$dA = 2\pi a(z) ds = 2\pi a(z) dz / \cos(\alpha(z)) \quad (6)$$

The radiation from a simple source is simply:

$$p = (\rho \exp(ikr) / 4\pi r) \dot{S} \Big|_{r=a} \quad (7)$$

⁸Skudrzyk, p. 459, eq. 14, 15, and 16.

where p is the acoustic pressure, ρ is the ambient density, k is the wave number, r is the distance from the source to the point of observation, and S is the volume velocity ($\dot{S} = dS/dt$). The incremental volume velocity for an element of length dz is given by $dS(z) = u_n(z) dA(z)$, and using (3), (6), and (7), the incremental pressure for that element is:

$$dp = (-i\rho\omega\exp(ikr)/2r) a(z) \left[u_r(z) + u_z(z) \tan(\alpha(z)) \right] dz \quad (8)$$

adopting $\exp(-i\omega t)$ time dependence.

For the far field approximation, small differences in range are ignored in the magnitude term, but retained in the phase. Hence, if $r = R - z \cos\theta$, where R ($R \gg L$) is the distance from the center of the body and θ is the angle with the z axis, the total pressure is expressed as:

$$p = -(i\rho\omega\exp(ikR)D/2R) \int_{-L/2}^{+L/2} \exp(-ikz \cos(\theta)) \left(\frac{1}{4} - (z/L)^2 \right)^{1/2} \\ \times \left(u_r(z) + \frac{u_z(z) D z}{L^2 \left(\frac{1}{4} - (z/L)^2 \right)^{1/2}} \right) dz \quad (9)$$

where use has been made of (1), (2), and (8).

The accordion mode of vibration is the fundamental, axial, elastic mode, with maximum velocity at the ends, no axial velocity at the center, and a lateral ("radial") velocity due to Poisson effect. This lateral velocity is maximum at the center. For a uniform tube, the ratio of lateral to axial velocity is $-\pi\sigma D/2L$, where σ is Poisson's ratio. Therefore, for a thin spheroidal shell, a fair approximation to the motion of the accordion mode is:⁹

⁹Chertock, p. 875.

$$u_z(z) = U_0 \sin(\pi z/L) \quad (10a)$$

$$u_r(z) = -(\pi\sigma D/2L)U_0 \cos(\pi z/L) \quad (10b)$$

Substituting these expressions into (9) yields the following expression for non-dimensional pressure \bar{P}_0 ,

$$\bar{P}_0 = \frac{PR}{(\exp(ikR)(-i\omega U_0)\rho(D/2)^2)} = I_1 + I_2 \quad (11)$$

where:

$$I_1 = 2/L^2 \int_{-L/2}^{+L/2} \exp(-ikz \cos(\theta)) z \sin(\pi z/L) dz$$

$$I_2 = -\pi\sigma/L \int_{-L/2}^{-L/2} \left(\frac{1}{4} - (z/L)^2\right)^{1/2} \exp(-ikz \cos(\theta)) \cos(\pi z/L) dz$$

Both integrals can be evaluated in closed form, thereby yielding:^{10,11}

$$I_1 = (w^2 - v^2)^{-2} \left[w(w^2 - v^2) \sin(w) + (w^2 + v^2) \cos(w) \right] \quad (12)$$

$$I_2 = (-\pi^2\sigma/8) \left(\frac{J_1(w-v)}{(w-v)} + \frac{J_1(w+v)}{(w+v)} \right)$$

where $w = kL \cos(\theta)/2$, $v = \pi/2$, and J_1 is the Bessel function of the first kind, of order 1. I_1 agrees exactly with Strasberg's result, but he has assumed $\sigma = 0$, so that $u_r = 0$, $I_2 = 0$ for his analysis. Combining (10), (11), and (12) leads to the desired expression for the total sound radiated by a spheroid in accordion mode vibrations:

¹⁰ Gradshteyn, p. 198, eq. 5.

¹¹ Abramowitz, p. 360, eq. 9.1.20., and p. 225, eq. 6.1.9.

$$\bar{P}_0 = (w^2 - v^2)^{-2} \left[w(w^2 - v^2) \sin(w) + (w^2 + v^2) \cos(w) \right]$$

$$- (\pi^2 \sigma / 8) \left(\frac{J_1(w-v)}{(w-v)} + \frac{J_1(w+v)}{(w+v)} \right)$$

Evaluation of this expression gives the smooth curve on Figures 1 and 2. In numerical calculation, care must be exercised to maintain precision in the region where w approaches v ($w = v + \epsilon$), since terms of order ϵ^2 must be retained within the parentheses to avoid a fictitious peak in the curve. If precision is maintained, the first expression converges to a finite value for $w = v$. The curves for I_1 and I_2 are plotted separately in the graph to allow individual comparison with spheroidal predictions and Strasberg's results.

For calculation of I_2 , a Poisson's ratio of .29 was used, which is the static value for a uniform steel shell. However, in practice, the value used would probably be modified by the addition of stiffeners to the shell and by dynamic effects of ring resonances at higher frequencies. Since the same value was used in both calculations, these modifications have no effect on the results here.

IV. Accordion Mode Spheroidal Calculation

The spheroidal wave function equivalent of the preceding expression will now be evaluated using the spheroidal functions that are outlined in Appendix A. For purposes of brevity, the abbreviated symbols S_{mn} and R_{mn} will be used to indicate the complete variables $S_{mn}(h, \eta)$ and $R_{mn}^{(3)}(h, \xi)$. $R_{mn}|_{\xi_0}$ will be used to indicate $R_{mn}^{(3)}(h, \xi_0)$ evaluated on the surface of the radiator.

The total acoustic pressure is the sum of the pressure contributions from each of the individual modes. If \bar{p}_{mn} are the modal spheroidal pressure coefficients, then:

$$p = \sum_m \sum_n \bar{p}_{mn} R_{mn} S_{mn} \cos(m\phi) \quad (13)$$

The relationship between pressure and the normal component of particle velocity is given by:¹²

$$\frac{\partial p}{\partial n} = \frac{1}{g_\xi} \frac{\partial p}{\partial \xi} = -\rho \frac{\partial u_n}{\partial t} = i\omega\rho u_n$$

where g_ξ is the metric coefficient.¹³ Therefore:

$$\sum_m \sum_n \bar{p}_{mn} R'_{mn} S_{mn} \cos(m\phi) = i\omega\rho u_n(\eta, \phi) g_\xi \quad (14)$$

where $R'_{mn} = \partial R_{mn} / \partial \xi$. If this equation is applied as a boundary condition over the surface of the radiator, the orthogonality of the angle functions can be utilized. Multiplying both sides of (14),

¹²Skudrzyk, p. 467.

¹³Skudrzyk, p. 459, eq. 18.

evaluated on $\xi = \xi_0$, by $S_{kl} \cos(k\phi)$ and integrating over the surface yields:

$$\sum_m \sum_n \bar{P}_{mn} R'_{mn} \Big|_{\xi_0} \int_0^{2\pi} \int_{-1}^{+1} S_{mn} \cos(m\phi) S_{kl} \cos(k\phi) d\eta d\phi$$

$$= i\omega p \int_0^{2\pi} \int_{-1}^{+1} g_{\xi_0} u_n(\eta, \phi) \Big|_{\xi_0} S_{kl} \cos(k\phi) d\eta d\phi \quad (15)$$

The integral¹⁴ on the left hand side of the above equation reduces to a multiple of the normalization constant and vanishes unless $m = k$ and $n = l$. The only non-zero value is $2\pi N_{mn} / \epsilon_m$, where $\epsilon_0 = 1$ and $\epsilon_m = 2$ for $m \neq 0$, and N_{mn} is given by equation (A.3).

Combining (13) and (15) and making use of (A.2) leads to the following expression:

$$p = (i\omega p d / 4\pi) \sum_m \sum_n \frac{\epsilon_m R_{mn} S_{mn} \cos(m\phi)}{N_{mn} R'_{mn} \Big|_{\xi_0}}$$

$$\times \sum_{r=0,1}^{\infty} d_r^{mn} \int_0^{2\pi} \int_{-1}^{+1} \left[\frac{\xi_0^2 - \eta^2}{\xi_0^2 - 1} \right]^{1/2} u_n \Big|_{\xi_0} P_{m+r}^m(\eta) \cos(m\phi) d\eta d\phi \quad (16)$$

which agrees with Chertock.¹⁵

For the accordion mode, the spheroidal modes that contribute to the radiation are the $m = 0$ and $n = \text{even}$ modes, since such vibration

¹⁴Skudrzyk, p. 470, eq. 56.

¹⁵Chertock, p. 873, eq. 12c and 13.

is independent of ϕ and symmetric about the midsection. Combining (16), (A.4), (A.5a), and (A.5b) with long, thin spheroid ($d \rightarrow L$) and far field ($\xi \rightarrow 2R/L, \eta \rightarrow \cos\theta$) approximations and integrating over ϕ leads to:

$$p = (\omega \rho L^2 \exp(ikR)/4R) \sum_{\substack{n=0 \\ \text{even}}}^{\infty} (d_{0n}^{On} i^{-(n+1)} S_{On} 2^n ((n/2)!)^2 (\xi_0^2 - 1)) / N_{On} n! \\ \times \sum_{\substack{r=0 \\ \text{even}}}^{\infty} d_r^{on} \int_{-1}^{+1} \left[\frac{\xi_0^2 - \eta^2}{\xi_0^2 - 1} \right]^{1/2} u_n(\eta) \Big|_{\xi_0} P_r(\eta) d\eta \quad (17)$$

An expression for the normal velocity on the surface can be derived from (3), (4), and (5) in spheroidal coordinates and is given by:

$$u_n(\eta) = U_0 \left[\frac{\xi_0^2 - 1}{\xi_0^2 - \eta^2} \right]^{1/2} \left[\eta \sin(\pi\eta/2) - (\pi\sigma/2) (1 - \eta^2)^{1/2} \cos(\pi\eta/2) \right] \quad (18)$$

which agrees with Chertock.¹⁶ Combining (17) and (18) and using the earlier definition of \bar{P}_0 (equation (11)), then:

$$\bar{P}_0 = \sum_{\substack{n=0 \\ \text{even}}}^{\infty} (d_{0n}^{On} \sin((n+1)\pi/2) S_{On} 2^n ((n/2)!)^2 / N_{On} n! \\ \times \sum_{\substack{r=0 \\ \text{even}}}^{\infty} d_r^{On} (J_r - (\pi\sigma/2) K_r) \quad (19)$$

¹⁶Chertock, p. 876, eq. 32.

where:

$$J_r = \int_{-1}^{+1} \eta \sin(\pi\eta/2) P_r(\eta) d\eta$$

$$K_r = \int_{-1}^{+1} (1 - \eta^2)^{1/2} \cos(\pi\eta/2) P_r(\eta) d\eta$$

The integral terms J_r and K_r were then evaluated for $r = 0, 2, 4$ by expansion of the Legendre polynomials and doing the resultant groups of integrals. Both groups are integrable in closed form, but the K_r series results in Bessel functions of the first kind of order $r/2 + 1$, which makes their evaluation somewhat cumbersome. The resultant values are:

r	J_r	K_r
0	.81057	1.1337
2	.28567	-.2970
4	-.02763	.0376

Utilizing the above values and tabulated data on the spheroidal functions, equation (19) can be used to determine \bar{P}_0 . It should be noted that the expansion coefficients (d_r^{On}) in (19) are those given by Flammer. If the wider range of Stratton's tables is desired, the difference in normalization¹⁷ must be accounted for. For use with Stratton's tables, equation (19) becomes:

¹⁷Flammer, p. 86.

$$\bar{P}_0 = \sum_{n=0}^{\infty} \frac{d_0(h|On) \left(\sum_{r=0}^{\infty} d_r(h|On) P_r(\eta) \right) \sum_{r=0}^{\infty} d_r(h|On) (J_r - (\pi\sigma/2)K_r)}{G_{On} H_{On}}$$

$$G_{On} = \sum_{r=0}^{\infty} 2(d_r(h|On))^2 / (2r + 1)$$

$$H_{On} = \sum_{r=0}^{\infty} (-1)^{1/2r} r! d_r(h|On) / 2^r ((r/2)!)^2$$

In this case, Stratton's tables were used with the above equation and excellent agreement with the approximation was achieved (as shown by the crosses on figures 1 and 2 and as demonstrated by Table I.) Calculations using Flammer's tables and equation (19) also demonstrated the approximation's accuracy.

FIGURE I
ACCORDION MODE PRESSURE
vs FREQUENCY

— Approximation
× Exact(Stratton)

\bar{P}_0
I₁ or J
Term

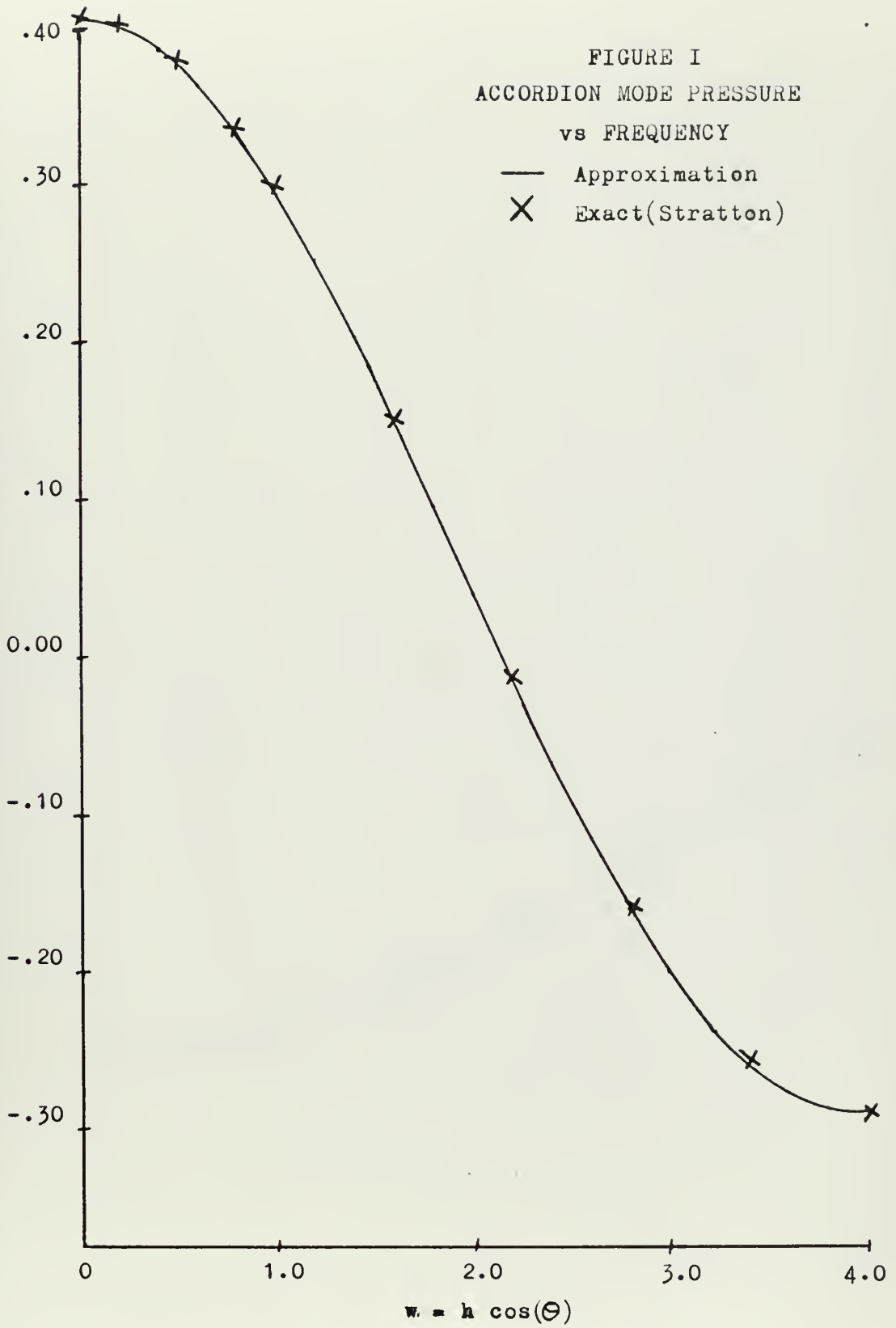


FIGURE 2
 ACCORDION MODE PRESSURE
 vs FREQUENCY

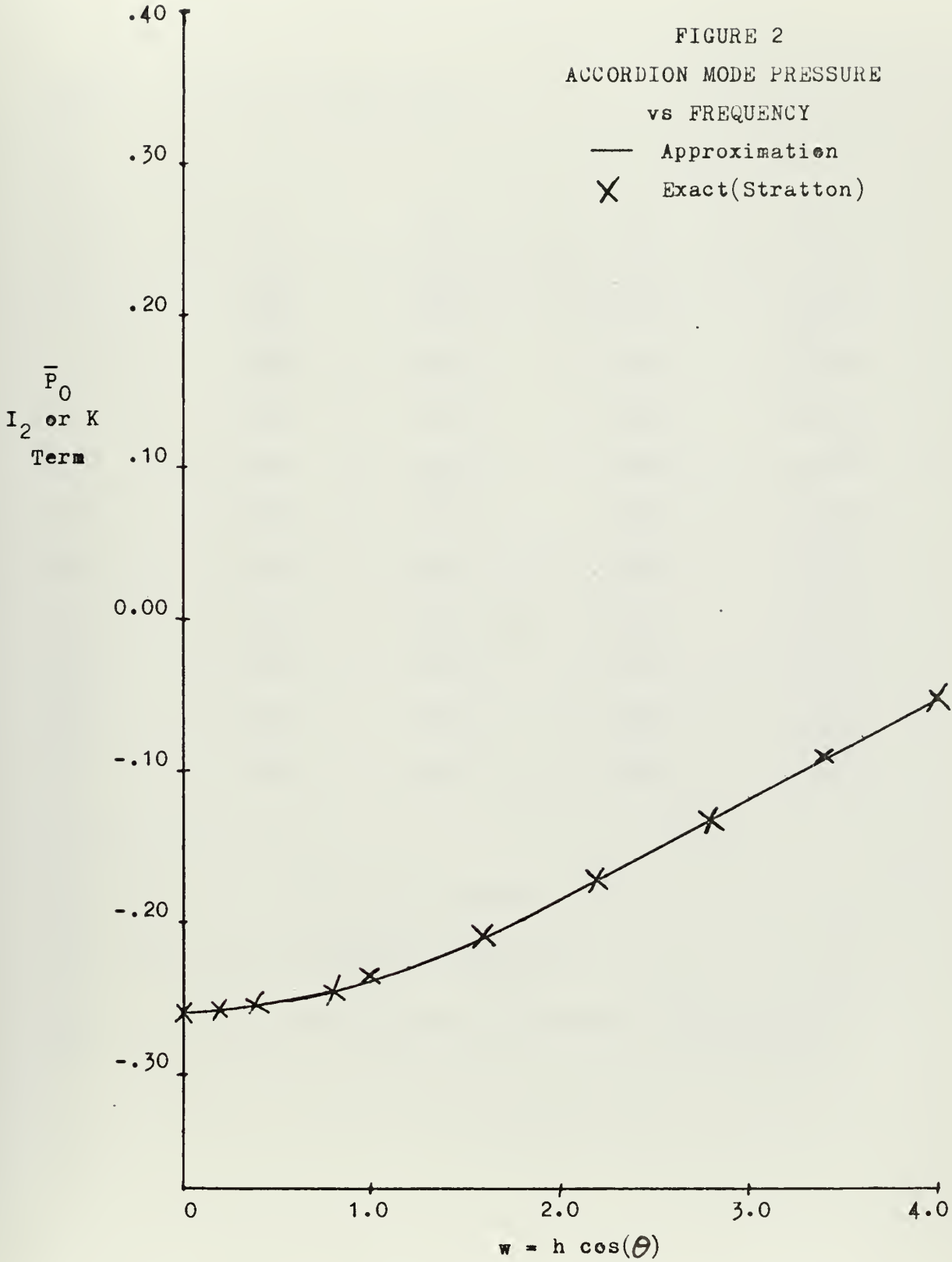


TABLE I - Accordion Mode Results

w	I_{1a}	I_{1s}	I_{2a}	I_{2s}
0	.4052	.4053	-.2582	-.2582
.20	.4007	.4007	-.2574	-.2574
.50	.3769	.3769	-.2530	-.2531
.80	.3343	.3343	-.2454	-.2454
1.00	.2966	.2928	-.2383	-.2358
1.60	.1515	.1513	-.2097	-.2096
2.20	-.0143	-.0169	-.1725	-.1725
2.80	-.1619	-.1620	-.1313	-.1313
3.40	-.2596	-.2591	-.0905	-.0902
4.40	-.2896	-.2895	-.0540	-.0542

I_{1a} - First term of array approximation

I_{1s} - First term of spheroidal prediction

I_{2a} , I_{2s} - Second terms of array and spheroidal, respectively.

V, Whipping Mode Approximation

The whipping mode is the beamlike transverse vibration of the shell. Since a slender spheroidal shape is again assumed, the properties derived in section III are applicable. The radiation from an element of length dz of the spheroid can be developed from the expression for a circular cylinder given by Junger and Feit.¹⁸ For such an element, the $n = 1$ term is:

$$p = (\rho a \exp(ikR)/R) (2\ddot{W}_1 \tilde{f}(k \cos(\theta)) (-i) (ka \sin\theta) \cos\phi/4$$

where:

$$\tilde{f}(k \cos\theta) = \int_Z^{Z+dZ} \cos(kz \cos\theta) dz = dz$$

Therefore:

$$dp = -\omega u_r(z) \rho \pi (a(z))^2 \exp(ikR) \sin\theta \cos\phi dz/R\lambda \quad (20)$$

which agrees with Junger.¹⁹

A transverse velocity distribution of the form $U_1(\cos(\pi z/L) - 2/\pi)$ would be the simplest vibratory mode of a uniform free-free beam.²⁰ For a slender spheroidal thin shell, very little error is introduced by using that velocity distribution. Substituting into (20) and using (1) and the phase difference term leads to:

¹⁸ Junger and Feit, p. 215.

¹⁹ Junger, p. 332.

²⁰ Den Hartog, p. 154.

$$\bar{P}_1 = - \frac{pR\lambda}{\omega U_1 L \rho \pi D^2 \exp(ikR) \cos(\phi)} = (I_3 + I_4 + I_5 + I_6) \sin(\theta)$$

$$I_3 = (1/4L) \int_{-L/2}^{L/2} \cos(\pi z/L) \exp(-ikz \cos\phi) dz$$

$$I_4 = -(1/L^3) \int_{-L/2}^{L/2} z^2 \cos(\pi z/L) \exp(-ikz \cos\theta) dz$$

$$I_5 = -(1/2\pi L) \int_{-L/2}^{L/2} \exp(-ikz \cos\theta) dz$$

$$I_6 = (2/\pi L^3) \int_{-L/2}^{L/2} z^2 \exp(-ikz \cos\theta) dz$$

All four integrals can be evaluated²¹ in closed form, yielding:

$$I_3 = \pi \cos(w) / 8 (v^2 - w^2)$$

$$I_4 = 8\pi \left[\cos(w) (6w^2 + 2v^2 - (v^2 - w^2)^2) - 4w \sin(w) (v^2 - w^2) \right] (v^2 - w^2)^{-3}$$

$$I_5 = -\sin(w) / 2\pi w$$

$$I_6 = (w \cos(w) + \sin(w) (w^2/2 - 1)) / \pi w^3$$

²¹ Gradshteyn, p. 198, eq. 8.

Combining the above expressions leads to the desired approximation:

$$\bar{P}_1 = \left[(v/2) (v^2 - w^2)^{-3} (\cos(w) (3w^2 + v^2) - 2w \sin(w) (v^2 - w^2)) \right. \\ \left. - \sin(w)/2\pi w + (w \cos(w) + \sin(w) (w^2/2 - 1))/\pi w^3 \right] \sin\theta$$

Numerical evaluation of this expression for two different frequencies is presented as Figures 3 and 4. Once again, care must be used to maintain precision in the region where w approaches v . In this case, the numerator of the first term must be evaluated to terms of order ϵ^4 to avoid a fictitious infinity.

VI. Whipping Mode Spheroidal Calculation

Calculation of the radiation from whipping mode vibration using spheroidal wave functions makes use of the basic relationships developed in section IV. Equation (16) is the general expression for all modes which is specialized to the whipping mode.

For the assumed whipping velocity distribution, the spheroidal modes contributing to the radiation are the $m = 1$ and symmetric modes. For $m = 1$, the symmetric modes are for $n - m$ even, or 11, 13, etc. The complete expression for the normal velocity on the surface is given by:

$$u_n(z, \phi) = u_r(z) \cos(\alpha(z)) \cos\phi$$

By making use of (5) and shifting to spheroidal coordinates, that expression becomes:

$$u_n(\eta, \phi) = (LU_1/D) (\cos(\pi\eta/2) - 2/\pi) \left(\frac{\xi_o^2 - 1}{\xi_o^2 - \eta^2} \right)^{1/2} (1 - \eta^2)^{1/2} \cos\phi \quad (21)$$

Combining (21) and (16) with (A.4), (A.5a), (A.5c), (A.5d) and long, thin spheroid ($d \gg L$) and far field ($\xi \rightarrow 2R/L$, $\eta \rightarrow \cos\theta$) and integrating over ϕ leads to:

$$\bar{P}_1 = -(1/4h^2) \sum_{n=1}^{\infty} \frac{-i^{-(n+1)} S_{1n} 2^n ((n-1)/2)! ((n+1)/2)! d_{-2}^{1n} B_{1n} A_{1n}}{N_{1n} (n+1)! C_{1n}} \quad (22)$$

where:

$$\begin{aligned}
A_{1n} &= \sum_{r=0}^{\infty} d_r^{1n} \int_{-1}^{+1} (1-\eta^2)^{1/2} (\cos(\pi\eta/2) - 2/\pi) P_{r+1}^1(\eta) d\eta \\
&= \sum_{r=0}^{\infty} d_r^{1n} \int_{-1}^{+1} (1-\eta^2) (\cos(\pi\eta/2) - 2/\pi) \frac{d}{d\eta} (P_{r+1}(\eta)) d\eta \\
B_{1n} &= \sum_{r=0}^{\infty} (r+2)(r+1) d_r^{1n} \\
C_{1n} &= \sum_{r=0}^{\infty} d_r^{1n}
\end{aligned}$$

which has been non-dimensionalized by multiplication by $1 = \pi h L / \lambda h^2$ and use has been made of the relationship:²²

$$P_{r+1}^1 = (1 - \eta^2)^{1/2} \frac{d}{d\eta} P_{r+1}$$

The integrals in A_{1n} can be evaluated using the same method used in the accordion mode section: expanding the Legendre polynomials and integrating. The values from those operations are:

$$r = 0, \quad .183223$$

$$r = 2, \quad -.490870$$

$$r = 4, \quad .031939$$

In this case, the pressure was evaluated using Flammer's tables over the same range of frequency. Figures 3 and 4 are marked with crosses indicating the spheroidal prediction from $h = 2$ and 4 over a quadrant

²²Hildebrand, p. 165, eq. 172.

of θ variation. As with the accordion mode, the line array correlates very closely with the spheroidal results. Table II gives numerical results for comparison.

FIGURE 3
WHIPPING MODE PRESSURE
vs ANGLE

$h = 2$

— Approximation
X Exact(Flammer)

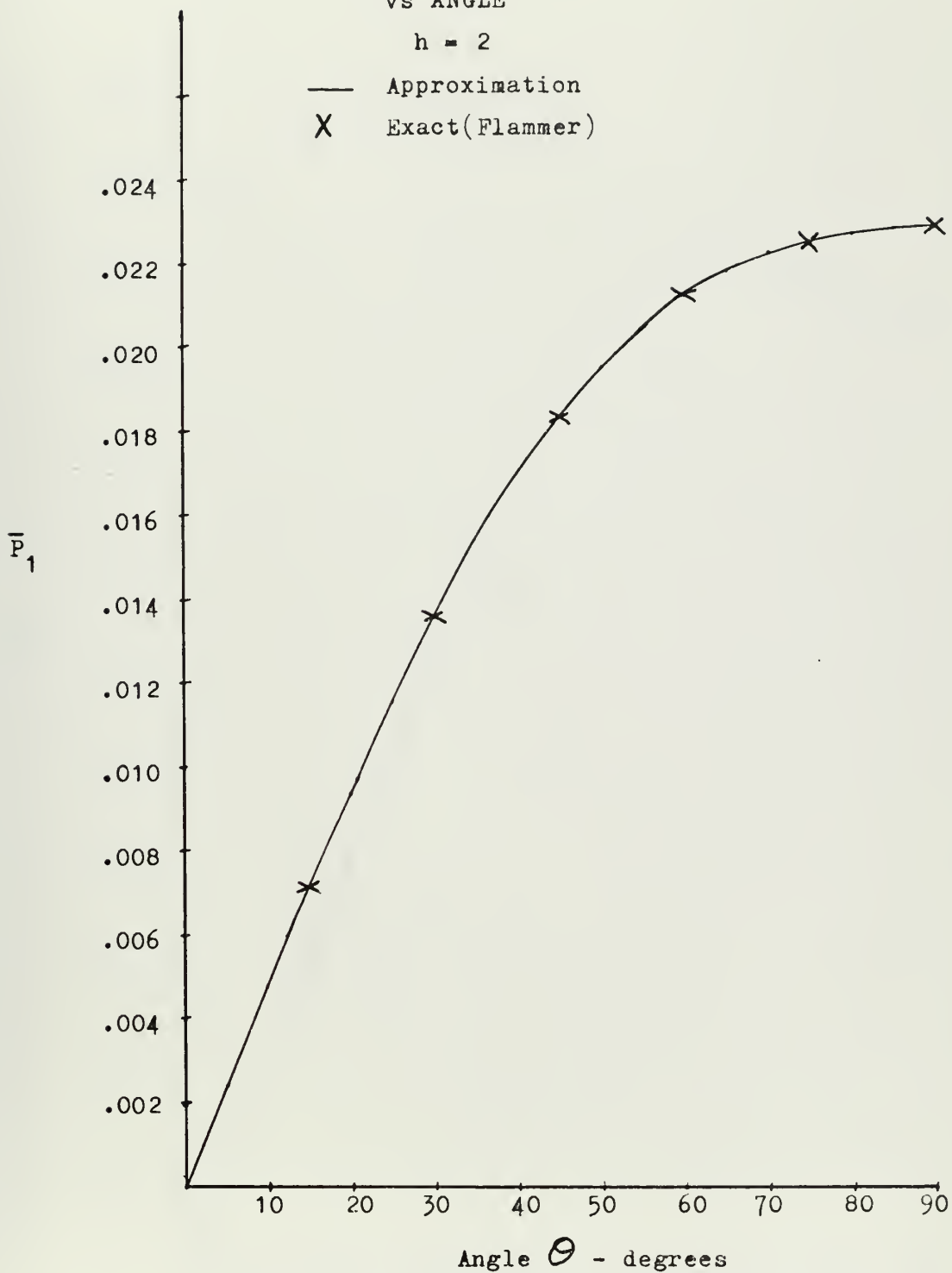


FIGURE 4
WHIPPING MODE PRESSURE

vs ANGLE

$h = 4$

— Approximation
X Exact(Flammer)

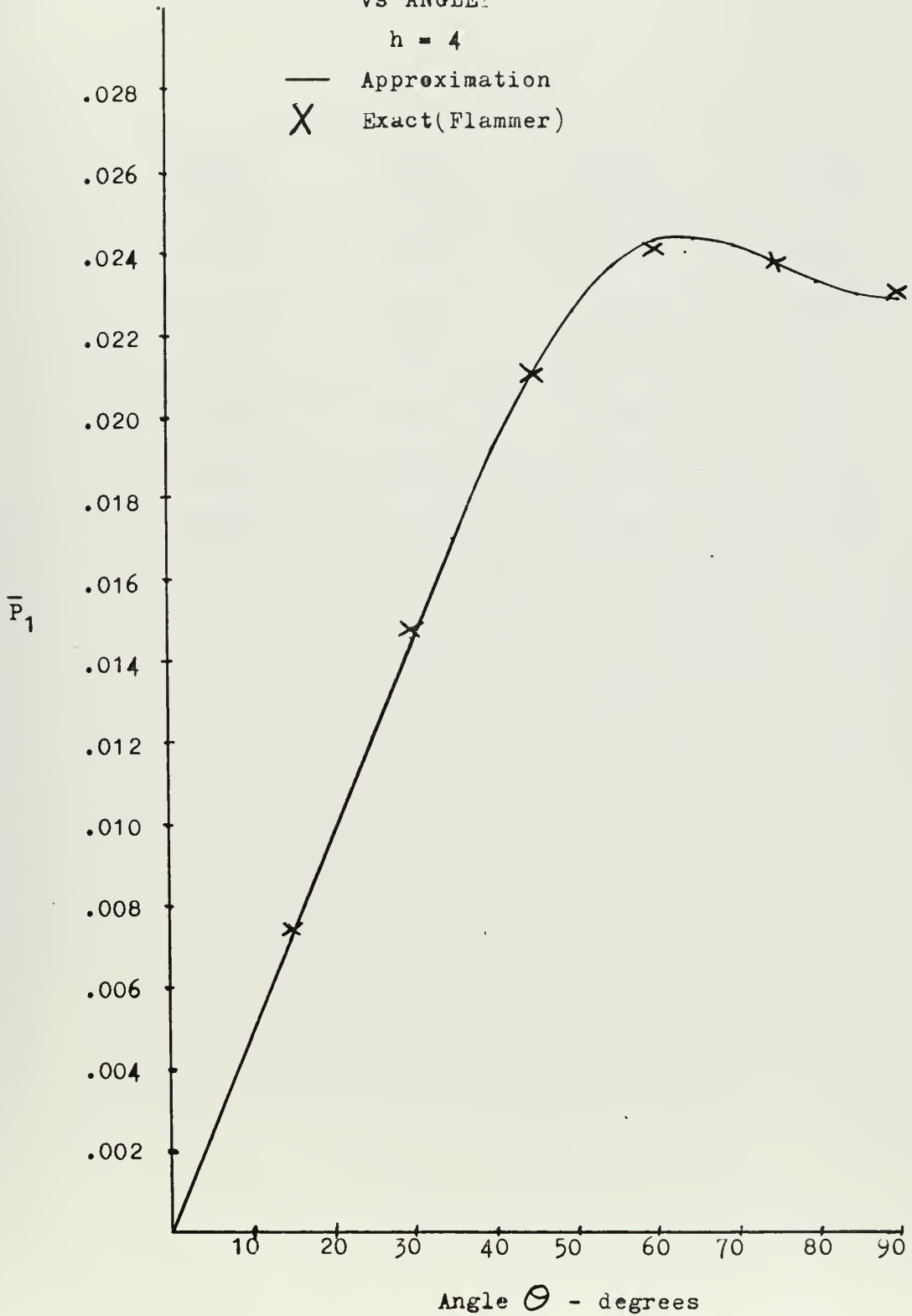


TABLE II - Whipping Mode Results

θ	$\bar{P}_1(h=2)$ Approx	$\bar{P}_1(h=2)$ Exact	$\bar{P}_1(h=4)$ Approx	$\bar{P}_1(h=4)$ Exact
15	.00720	.00720	.00721	.00739
30	.01355	.01356	.01466	.01484
45	.01836	.01836	.02112	.02111
60	.02127	.02127	.02430	.02417
75	.02258	.02257	.02383	.02384
90	.02290	.02290	.02290	.02303

VII Near Field Approximations

The most severe restriction assumed in the derivation of these expressions is the far-field approximations. These approximations simplify the evaluation of the expressions and permit solution in closed form. However, practical considerations encourage the development of models that can be used at observation locations closer to the radiator. Therefore, the evaluation of the approximations was extended to the near field. Time constraints permitted such evaluation for beam aspect at $h = 2$ only. However, the computer program developed has purposely been kept general and can be used for any position or frequency.

In the prior derivations, the far-field assumption permitted extraction outside the integral of the exponential and range terms (Equation (8) to equation (9) and application of equation (20)). Retaining these terms within the integral leads to integrals that are practically impossible to evaluate in closed form. Therefore, numerical evaluation was selected, and a computer program was developed. The integrals so evaluated are:

$$\bar{P}_0 = \text{DIST} \int_{-1/2}^{+1/2} \frac{\exp(ikR)}{R} \left[\bar{z} \sin(\pi\bar{z}) - \frac{\pi\sigma}{2} (1/4 - \bar{z}^2)^{1/2} \cos(\pi\bar{z}) \right] d\bar{z}$$

for the accordion mode, where $\bar{z} = z/L$ and $\text{DIST} = R/L$; and

$$\bar{P}_1 = \text{DIST} \int_{-1/2}^{+1/2} \frac{\exp(ikR) \overline{RF}}{R^2} (\cos(\pi\bar{z}) - 2/\pi) \left(\frac{1}{4} - \bar{z}^2 \right) d\bar{z}$$

for the whipping mode, where \overline{RF} = Distance Abeam/Length. In both cases R must be retained as a function of Z for near field results. The computer program calculates and sums the real and imaginary contributions from each segment of length $d\overline{Z}$ along the body and then calculates the magnitude of the pressure term. A listing of the program is included in Appendix B. In all cases, convergence to less than 1.9% was required, but in most calculations, the convergence was considerably better. For all whipping calculations, convergence was less than 0.04%.

The spheroidal values for the near field pressure magnitudes were calculated using the following expressions, which were derived from equations (19) and (22) for beam aspect ($\theta = 90^\circ$):

$$\overline{P}_0 = h \text{ DIST} \left[(.127R_{00}^{(1)} - .168R_{02}^{(1)})^2 + (.127R_{00}^{(2)} - .168R_{02}^{(2)})^2 \right]^{1/2}$$

$$\overline{P}_1 = \text{DIST}/h \left[(.206R_{11}^{(1)} + .022R_{13}^{(1)})^2 + (.206R_{11}^{(2)} + .022R_{13}^{(2)})^2 \right]^{1/2}$$

Values for the radial spheroidal functions were obtained from the NRL tables,²³ which give only limited data for values of ξ greater than 1.4. For both modes, only the first two spheroidal harmonics were used: 00 and 02 for accordion and 11 and 13 for whipping.

The values calculated for both the approximations (solid curve) and spheroidal expressions (crosses) are shown in Figures 5 and 6 and Table III. The far field computer results for both modes agree with solutions of prior sections. The agreement for the accordion mode is extremely good to a distance of a quarter-length abeam. The

²³Hanish, S., et al., Tables of Radial Spheroidal Wave Functions, NRL Report 7088 (Washington, 1970).

whipping mode is not as good and can be useful to a minimum distance of about half-length. Since convergence for whipping numerical calculations is very good, this error can be attributed to a combination of inherent inaccuracy of the model and the possible inaccuracy introduced by truncating the spheroidal evaluation at only two terms. Therefore, in view of the possible inaccuracies of each solution individually and the variation between them, neither near field whipping mode solution should be considered the exact or correct solution.

FIGURE 5
 ACCORDION MODE PRESSURE
 vs DISTANCE

— Approximation
 X Exact(Flammer, Hanish)
 $h = 2$

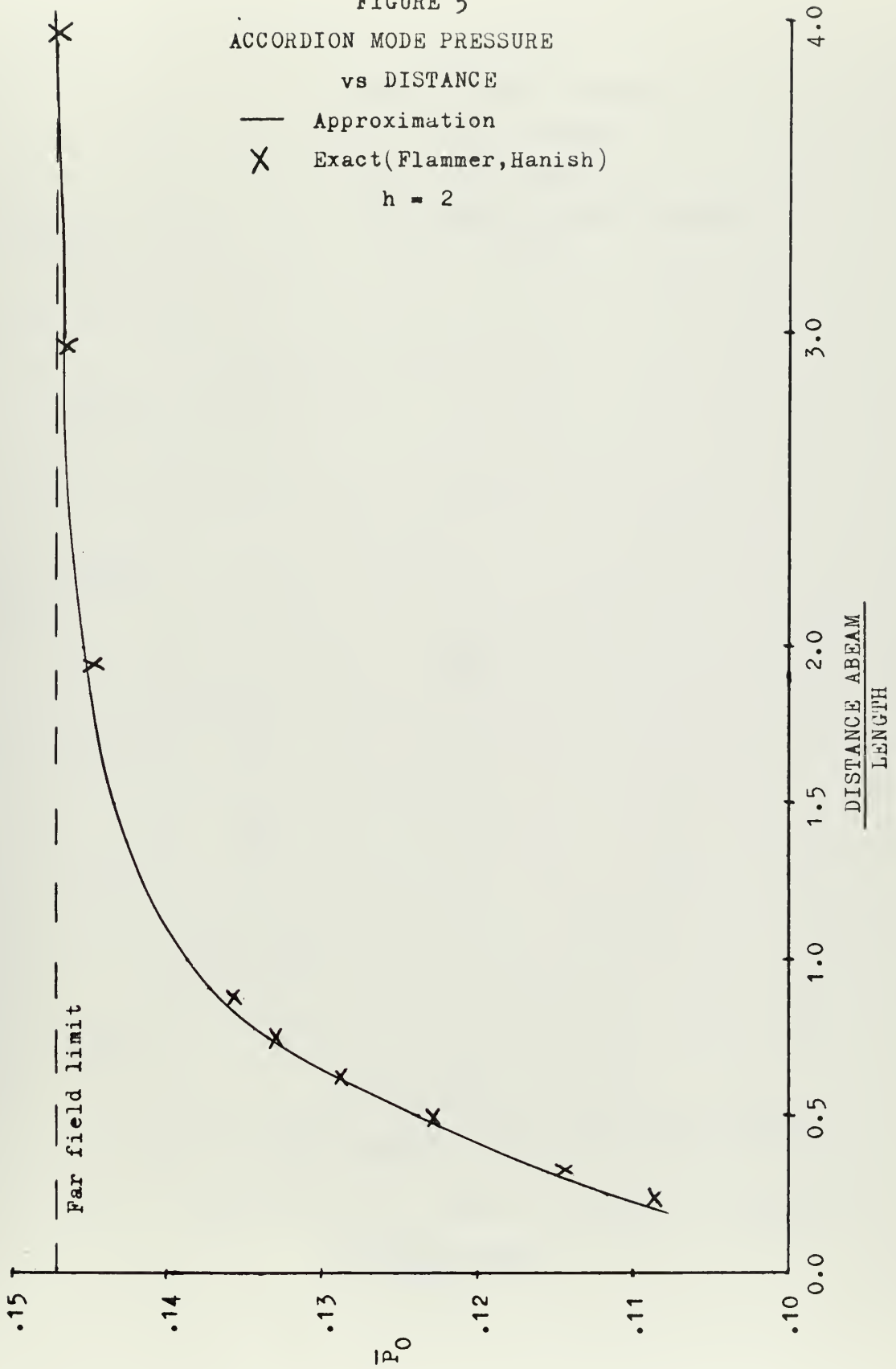


FIGURE 6
WHIPPING MODE PRESSURE

vs DISTANCE

— Approximation

X Exact(Flammer, Hanish)

$h = 2$

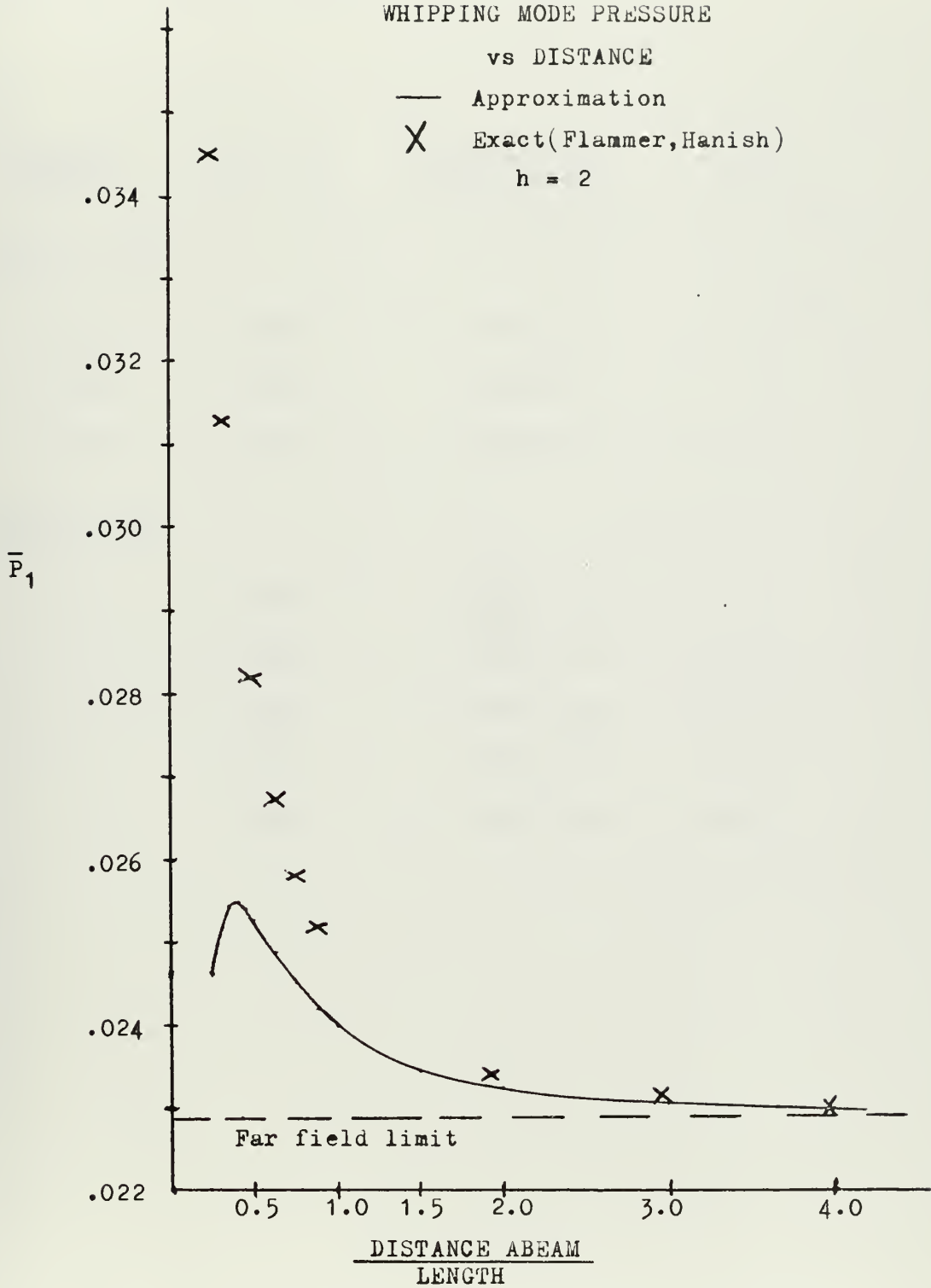


TABLE III - Near Field Results

<u>Distance</u> <u>Length</u>	Spheroidal	Approximation (Convergence (%))	Error(%)
Accordion Mode			
2.00	.1446	.1453 (.65)	.48
.75	.1328	.1335 (.60)	.52
.50	.1230	.1239 (.40)	.73
Whipping Mode			
2.00	.02344	.02323 (.01)	1.89
.87	.02519	.02422 (.01)	3.80
.75	.02579	.02452 (.001)	4.90
.62	.02671	.02489 (.001)	6.80
.50	.02822	.02528 (.02)	10.40

VIII. Summary and Conclusions

This paper has developed an approximation for the sound radiation of two fundamental vibratory modes of a spheroidal body. This approximation has demonstrated very good correlation with the exact spheroidal prediction over the frequency range of practical interest. The expressions developed are far more straightforward than the cumbersome spheroidal wave functions. Their future use should therefore promote faster and easier predictions of such radiation.

The two obvious limitations of these approximations in practical application are the near field performance and the physical limitation imposed by a spheroidal shape. Section VII has demonstrated excellent near field performance for the accordion mode approximation and fairly good performance for the whipping mode, at least in the intermediate or "suburban" field. The second limitation of shape differences between a spheroid and actual physical radiators should not be severe, particularly since the actual shape can be incorporated into the approximation and evaluation carried out numerically.

Appendix A - Spheroidal Wave Functions

Spheroidal wave functions are the result of the solution of the wave equation in spheroidal coordinates by the usual technique of separation of variables. The prolate spheroidal coordinates that are of interest here are obtained by rotating elliptic coordinates about the major axis. If the foci of the ellipse are located at $(x, y, z) = (0, 0, \pm d/2)$ and r_1 and r_2 are the distances from these foci, then the spheroidal coordinates are:

$$\xi = (r_1 + r_2)/d \quad 1 \leq \xi < \infty$$

$$\eta = (r_1 - r_2)/d \quad -1 \leq \eta \leq +1$$

$$\phi = \tan^{-1}(y/x) \quad 0 \leq \phi < 2\pi$$

Surfaces of constant ξ are confocal ellipsoids; surfaces of constant η are confocal hyperboloids orthogonal to the ellipsoids. For a spheroid of length L and minor diameter D :

$$\xi^2 = 1 + D^2/d^2$$

An ellipse is defined by surfaces where $r_1 + r_2 = \text{constant}$. Hence, on the major axis, $r_1 + r_2 = L$, and on the minor axis, $r_1 + r_2 = 2((D/2)^2 + (d/2)^2)^{1/2}$. Therefore, $L^2 = D^2 + d^2$, and for $L \gg D$, or for a slender or needle shaped spheroid, $d \rightarrow L$. The radial coordinate on the surface, or ξ_0 , approaches 1 for slender spheroids.

In the far field, $r_1 + r_2 \rightarrow 2R$, and $\xi \rightarrow 2R/d$, where R is the average distance to the spheroid. Furthermore, in the far field, $\eta \rightarrow \cos(\theta)$, where θ is the angle with the major axis.

The separable solution is of the form:

$$P_{mn} = S_{mn}(h, \eta) R_{mn}(h, \xi) \cos(m\phi) \quad (\text{A.1})$$

where the indices m and n ($m \leq n$) identify the various modes. The parameter h is a non-dimensional frequency, $h = \frac{1}{2}\omega d/c = \frac{1}{2}kd$, where ω and c are the angular frequency and sound speed, and k is the wave number, or their ratio. A surface harmonic is represented by $S_{mn}(h, \eta) \cos(m\phi)$ which vanishes at $n-m$ circles of latitude.

Through application of the Laplacian operator in spheroidal coordinates to the above solution, it can be shown that both R_{mn} and S_{mn} satisfy the same ordinary differential equation.

$$\frac{d}{dz} \left[(1-z^2) \frac{du}{dz} \right] + \left[\lambda - h^2 z^2 - \frac{\mu^2}{1-z^2} \right] u = 0$$

where for $-1 \leq z \leq +1$, $z = \eta$ and $u = S_{mn}$

and for $+1 \leq z < \infty$, $z = \xi$ and $u = R_{mn}$

The angle functions $S_{mn}(h, \eta)$ are generalizations of Legendre functions and depend on m, n, h , and η , thereby making spheroidal manipulations cumbersome. They are generally expressed as series expansions of Legendre functions as follows:

$$S_{mn}(h, \eta) = \sum_{r=0,1}^{\infty} d_r^{mn}(h) P_{m+r}^m(\eta) \quad (\text{A.2})$$

where the prime over the summation sign indicates summation over only even values of r when $n-m$ is even, and over only odd values of r when

$n-m$ is odd. The expansion coefficients are available in Flammer and Stratton, although the range of the latter is much greater.

A quantity required for calculations is the norm or mean square, which is also a function of m, n , and h , and is given by:

$$N_{mn}(h) = \int_{-1}^{+1} (S_{mn}(h, \eta))^2 d\eta = 2 \sum_{r=0,1}^{\infty} \frac{(r+2m)! [d_r^{mn}(h)]^2}{r!(2r+2m+1)} \quad (\text{A.3})$$

This quantity is tabulated for limited ranges in Flammer, but must be calculated from the expansion coefficients in the use of Stratton's tables.

The radial function is a complex function describing the distance dependence of the wave functions. It may be computed at any point by a series expansion of spherical Hankel functions of the first kind. Additionally, numerous tables are in existence for a wide range of frequencies and distances. For time dependence $\exp(-i\omega t)$, which is used here, the radial solutions are:

$$R_{mn}^{(3)}(h, \xi) = R_{mn}^{(1)}(h, \xi) + iR_{mn}^{(2)}(h, \xi)$$

which correspond to the diverging wave.

However, for purposes of this study, only the far field approximations for long and thin spheroids are required. These are available in both Chertock¹ and Skudrzyk.² For $h\xi \gg 1$:

¹G. Chertock, p. 872-873.

²E. Skudrzyk, p. 464, p. 475-476.

$$R_{mn}^{(3)}(h, \xi) \rightarrow i^{-(n+1)} \exp(ih\xi) / (h\xi) \quad (\text{A.4})$$

Since $h = \frac{1}{2} kd$ and $\xi \rightarrow 2R/d$ in the far field, the exponential term becomes $\exp(ikR)$.

A further quantity required for the calculation of sound radiation is the derivative of the radial function. For slender spheroids:

$$R_{mn}^{(3)'}(h, \xi) = \frac{\partial}{\partial \xi} \left[R_{mn}^{(3)}(h, \xi) \right] \xrightarrow{\xi \rightarrow 1} i R_{mn}^{(2)'}(h, \xi) \quad (\text{A.5(a)})$$

For $m = 0$:

$$R_{on}^{(2)'}(h, \xi) \xrightarrow{\xi \rightarrow 1} \frac{n! (\xi^2 - 1)^{-1}}{2^n (n/2)! (n/2)! h d_{on}^{on}(h)} \quad n \text{ even} \quad (\text{A.5(b)})$$

For $m > 0$:

$$R_{mn}^{(2)'}(h, \xi) \xrightarrow{\xi \rightarrow 1} -m f_2(m, n, h) (\xi^2 - 1)^{-1/2m-1} \quad (\text{A.5(c)})$$

Where:

$$f_2(m, n, h) = \frac{(-1)^m (2m-1) (m-1)! (m+1)! h^{n-1} \sum_{r=-2m}^{\infty} d_r^{mn}(h)}{2^{n-2m+1} (2m)! \left(\frac{n-m}{2}\right)! \left(\frac{n+m}{2}\right)! d_{-2m}^{mn}(h) \sum_{r=0}^{\infty} \frac{(2m+r)!}{r!} d_r^{mn}(h)} \quad n \text{ even} \quad (\text{A.5(d)})$$

Appendix B

```

C READ IN INPUT
C RF IS DISTANCE ABEAM/LENGTH
C ZF IS DISTANCE FWD OF AMIDSHIPS/LENGTH
C H IS DIMENSIONLESS FREQUENCY
C DZ IS INITIAL INCREMENT
C XI,ETA ARE SPHEROIDAL COORDINATES
C CHECKS ARE PERCENTAGE CHANGE IN RESULT DUE TO INCREMENT REDUCTION
  READ(5,200) RF,ZF,H,DZ
  FORMAT(4F10.5)
  R1=SQRT(RF**2 + (.5 - ZF)**2)
  R2=SQRT(RF**2 + (.5 + ZF)**2)
  XI = R1 + R2
  ETA = R1 - R2
  DIST=SQRT(RF**2 + ZF**2)
  WRITE(6,211) DIST
211  FORMAT('1 DISTANCE FROM SOURCE IS ',F6.2,' TIMES LENGTH')
  WRITE(6,220) RF,ZF
220  FORMAT(' POSITION ',F6.2,' X L ABEAM AND ',F6.2,' X L OFF CL')
  WRITE(6,204) XI,ETA,H
204  FORMAT(' XI = ',F10.3,' ETA = ',F10.7,' H = ',F6.2)
  WRITE(6,214)
214  FORMAT('
INCREMENT REAL PART IMAGINARY REAL C
CHECK IMAGINARY CHECK')
  N=0
  TSTPA=0.0
  TSTUA=0.0
  TSTPW=0.0
  TSTUW=0.0
  PI=3.14159
  TPLAC=0.0
  TUNAC=0.0
  TRLWH=0.0
  TUNWH=0.0
201

```



```

R0=SQRT(RF**2 + (Z-ZF)**2)
FX=2.*H*RO
RLACC=COS(FX)/RO
UNACC=SIN(FX)/RO
RLWHQ=0.0
UNWHQ=0.0
Z=Z+D7
R=SQRT(RF**2+(Z-ZF)**2)
FX=2.*H*R
ARG=PI*7
A=ABS(.25-Z**2)
FAC=(7*SIN(ARG)-PI*.145*SQRT(A)*COS(ARG))*2./R
FWH=RF*(COS(ARG)-2./PI)*(.25-Z**2)/R**2
RLAC=FAC*COS(FX)
UNAC=FAC*SIN(FX)
RLWH=FWH*COS(FX)
UNWH=FWH*SIN(FX)
AVRLA=(RLACC+RLAC)*DZ/2.
AVUNA=(UNACC+UNAC)*DZ/2.
AVRLW=(RLWHQ+RLWH)*DZ/2.
AVUNW=(UNWHQ+UNWH)*DZ/2.
TP1AC=TRLAC+AVRLA
TUNAC=TUNAC+AVUNA
TRLWH=TRLWH+AVRLW
TUNWH=TUNWH+AVUNW
RLACC=RLAC
UNACC=UNAC
RLWHQ=RLWH
UNWHQ=UNWH
IF(7.LT.0.5) GO TO 202
CHRA=100.*ABS(ABS(TSTRA/TRLAC)-1.)
CHUA=100.*ABS(ABS(TSTUA/TUNAC)-1.)
CHRW=100.*ABS(ABS(TSTRW/TRLWH)-1.)
CHUW=100.*ABS(ABS(TSTUW/TUNWH)-1.)

```

202


```

WRITE(6,212) DZ,TRLAC,TUNAC,CHRA,CHUA
FORMAT(' ACCORDIAN MODE ',F10.8,2X,E11.4,1X,E11.4,2X,F7.2,5X,F7.2)
WRITE(6,213) DZ,TRLWH,TUNWH,CHRW,CHUW
FORMAT(' WHIPPING MODE ',F10.8,2X,E11.4,1X,E11.4,2X,F7.2,5X,F7.2)
TSTRA=TRLAC
TSTUA=TUNAC
TSTRK=TRLWH
TSTUW=TUNWH
IF(CHPA.LT.1.9.AND.CHUA.LT.1.9.AND.CHRW.LT.1.9.AND.CHUW.LT.1.9) GO
1 TO 206
C CONVERGENCE LIMITS, LESS THAN 1.9% RQUIRED
DZ=DZ/2.
N=N+1
IF(N.GT.3) GO TO 206
GO TO 201
206 ACC=DIST*SORT(TRLAC**2 + TUNAC**2)
WHIP=DIST*SORT(TRLWH**2 + TUNWH**2)
C ACC IS MAGNITUDE OF ACCORDION MODE PRESSURE
C WHIP IS MAGNITUDE OF WHIPPING MODE PRESSURE
WRITE(6,207) ACC,WHIP
207 FORMAT(' AMPLITUDES',/, ' ACCORDIAN ',E11.4,/, ' WHIPPING ',F11.4)
STOP
END
C
C
C SAMPLE INPUT DATA
C
0.50 0.0 2.0 .001
0.25 0.0 2.0 .001

```


Appendix C - Important Symbols

$a(z)$	radius of cross section
c	sound speed in medium
d	focal length
h	non-dimensional frequency = $\frac{1}{2}kd$
k	wave number = $2\pi/\lambda$
m, n, r	index
p	acoustic pressure
t	time
u_n, u_z, u_r	velocity components
v	$\pi/2$
w	$kL \cos(\theta)/2$
D	maximum diameter of spheroid
L	length of spheroid
$N_{mn}(h)$	normalization constant
$P_m^n(\eta)$	Legendre functions
\bar{P}_0	Accordion mode non-dimensional pressure
\bar{P}_1	Whipping mode non-dimensional pressure
R	Far field range
$R_{mn}(h, \xi)$	Radial spheroidal function
$S_{mn}(h, \eta)$	Angle spheroidal function
U_0	Maximum velocity, accordion
U_1	Maximum velocity, whipping
ξ	Radial coordinate
η	Angle coordinate
ϕ	Longitudinal angle
θ	Angle with axis

Appendix D - Bibliography

The following references were consulted:

1. Abramowitz, M. and Stegun, I.A., ed., Handbook of Mathematical Functions (National Bureau of Standards, 1970).
2. Blake, W. K., "Radiation From Free-Free Beams Under Influences of Light and Heavy Fluid Loading," NSRDC Report 3716(1971).
3. Chertock, G., "Sound Radiation from Prolate Spheroids," JASA 33(1961).
4. Den Hartog, J. P., Mechanical Vibrations (New York, 1956).
5. Flammer, C., Spheroidal Wave Functions (Stanford, 1957).
6. Gradshteyn, I. S. and Ryzhik, I. M., Table of Integrals, Series and Products (New York, 1965).
7. Hanish, S., et al., Tables of Radial Spheroidal Wave Functions, NRL Report 7088 (Washington, 1970).
8. Hildebrand, F. B., Advanced Calculus for Applications (Englewood Cliffs, N. J., 1962).
9. Junger, M. C., "Sound Radiation by Resonances of Free-Free Beams," JASA 52 (1972).
10. Junger, M. C. and Feit, D., Sound, Structures, and Their Interaction (Cambridge, Mass., 1972).
11. Morse, P. M. and Feshbach, H., Methods of Theoretical Physics (New York, 1953).
12. Morse, P. M. and Ingard, K. U., Theoretical Acoustics (New York, 1968).
13. Skudrzyk, E., The Foundations of Acoustics (New York, 1971).
14. Strasberg, M., "Sound Radiation from Slender Bodies in Axisymmetric Vibrations," Fourth International Congress on Acoustics, 1962.
15. Stratton, J. A., et al., Spheroidal Wave Functions (Cambridge, Mass., 1956).



Thesis
A3345 Akst

145674

Sound radiation from
line arrays.

16 OCT 73

DISPLAY.

Thesis
A3345 Akst

145674

Sound radiation from
line arrays.

thesA3345

Sound radiation from line arrays.



3 2768 001 90958 3

DUDLEY KNOX LIBRARY